iScience

CellPress
OPEN ACCESS

Article

Crosstalk between *vrille* transcripts, proteins, and regulatory elements controlling circadian rhythms and development in *Drosophila*

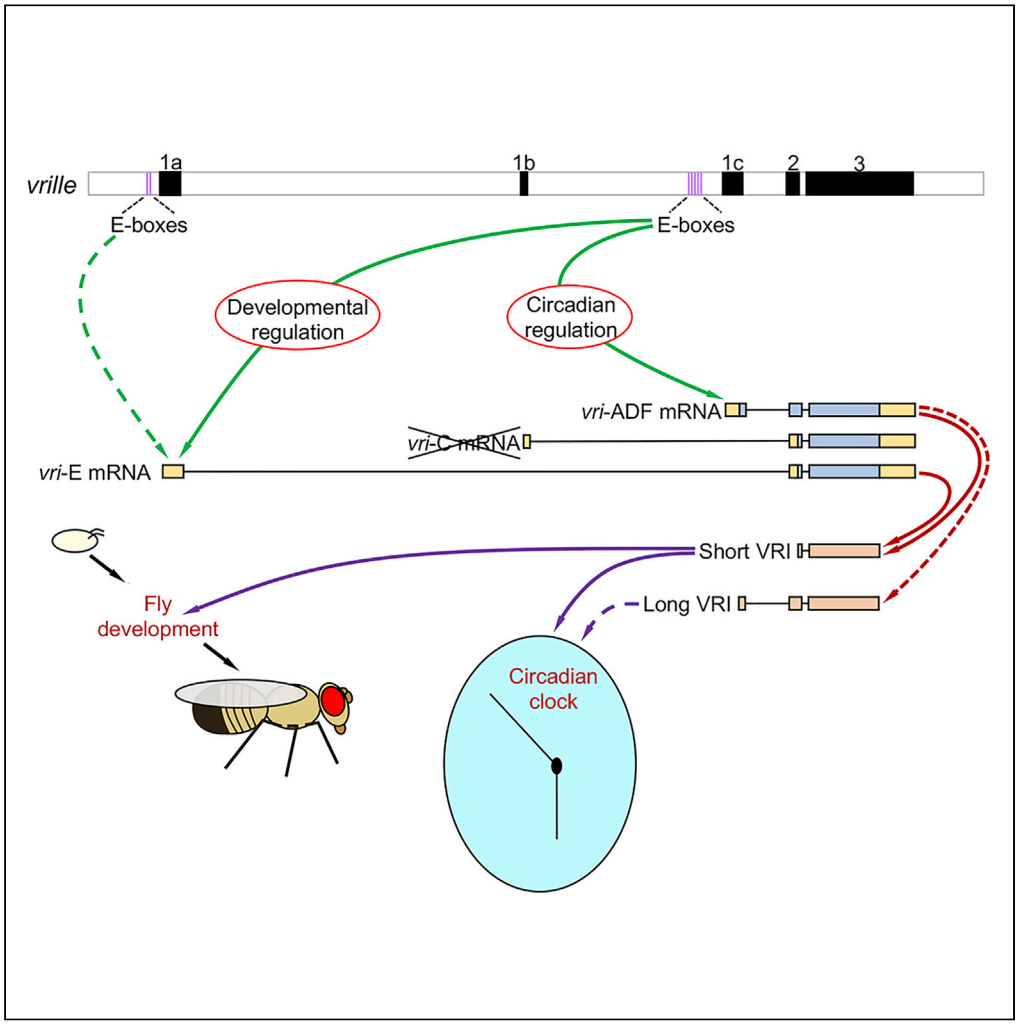

Kushan L. Gunawardhana, Gustavo B.S. Rivas, Courtney Caster, Paul E. Hardin

phardin@bio.tamu.edu

HIGHLIGHTS

vri-E mRNA is sufficient for *Drosophila* development and circadian behavior

E-boxes upstream of the *vri*-ADF promoter are required for *Drosophila* development

vri-ADF mRNAs primarily produce short VRI protein rather than long VRI protein

Short VRI protein primarily controls *Drosophila* development and circadian behavior

Gunawardhana et al., iScience *24*, 101893
January 22, 2021
https://doi.org/10.1016/j.isci.2020.101893

iScience

CellPress
OPEN ACCESS

Article

Crosstalk between *vrille* transcripts, proteins, and regulatory elements controlling circadian rhythms and development in *Drosophila*

Kushan L. Gunawardhana,[1] Gustavo B.S. Rivas,[1] Courtney Caster,[1] and Paul E. Hardin[1,2,*]

SUMMARY

The *vrille* (*vri*) gene encodes a transcriptional repressor required for *Drosophila* development as well as circadian behavior in adults. Alternate first exons produce *vri* transcripts predicted to produce a short VRI isoform during development and long VRI in adults. A *vri* mutant ($vri^{\Delta 679}$) lacking long VRI transcripts is viable, confirming that short VRI is sufficient for developmental functions, yet behavioral rhythms in $vri^{\Delta 679}$ flies persist, showing that short VRI is sufficient for clock output. E-box regulatory elements that drive rhythmic long VRI transcript expression are required for developmental expression of short VRI transcripts. Surprisingly, long VRI transcripts primarily produce short VRI in adults, apparently due to a poor Kozak sequence context, demonstrating that short VRI drives circadian behavior. Thus, E-box-driven long VRI transcripts primarily control circadian rhythms via short VRI, whereas the same E-boxes drive short VRI transcripts that control developmental functions using short VRI.

INTRODUCTION

The *vrille* (*vri*) gene from *Drosophila* encodes a bZIP transcriptional repressor that was initially identified as an enhancer of *decapentaplegic* (*dpp*) dorsoventral patterning defects (George and Terracol, 1997). *vri* null mutants show multiple embryo patterning defects that cause lethality before hatching as L1 larvae (George and Terracol, 1997), and patches of *vri* mutant tissue in adults show patterning and proliferation defects (George and Terracol, 1997; Szuplewski et al., 2003). Subsequently, *vri* was recovered in a screen for circadian clock-controlled transcripts present in adult heads (Blau and Young, 1999). As *vri* mutants are embryonic lethal, *vri* function in the clock was first characterized via overexpression, which lengthened or abolished behavioral rhythms (Blau and Young, 1999). Indeed, *vri* rhythmically represses transcription of the key clock activator *Clock* (*Clk*) as well as other genes whose mRNAs cycle with a peak around dawn (Cyran et al., 2003; Glossop et al., 2003; Hardin, 2011). Transgenic flies that permit conditional *vri* inactivation revealed that *vri* is not necessary for molecular clock function, but disrupts clock output in key brain pacemaker neurons to abolish behavioral rhythms (Gunawardhana and Hardin, 2017).

The *vri* gene produces two protein isoforms from five transcripts that are initiated at three different first exons (Gramates et al., 2017; Szuplewski et al., 2003). The 610-amino acid short VRI isoform (short VRI) is produced by the *vri*-E and *vri*-C transcripts that initiate at first exons 1a and 1b, respectively, whereas the 729-amino acid long isoform (long VRI) is produced by three transcripts that only differ in their 3′ UTR length, *vri*-A, *vri*-D, and *vri*-F (henceforth referred to as *vri*-ADF) initiated at first exon 1c. Each first exon splices onto common second and third exons to produce full-length mRNAs, but translation of *vri*-E and *vri*-C initiates within exon 2 to produce short VRI, whereas translation from *vri*-ADF initiates in exon 1c to produce long VRI. In adults, prominent ~85-kDa and minor >90-kDa VRI bands are rhythmically expressed, but migrate more slowly than the predicted ~65-kDa short and ~78-kDa long VRI isoforms (Glossop et al., 2003). The ~85- and >90-kDa VRI bands seen in wild-type adults likely correspond to short VRI and long VRI, respectively, but this predicted relationship has not been tested.

Mutants that eliminate transcription or translation of exons common to all *vri* transcripts are lethal (George and Terracol, 1997; Szuplewski et al., 2003). A 17-kb *vri* transgene that lacks only exon 1a fails to rescue developmental lethality, suggesting that the *vri*-E transcript is necessary for development (George and Terracol, 1997). Although RNA sequencing (RNA-seq) detects little if any *vri*-C mRNA, *vri*-E mRNA is detected

[1]Department of Biology and Center for Biological Clocks Research, Texas A&M University, College Station, TX, USA

[2]Lead contact

*Correspondence: phardin@bio.tamu.edu

https://doi.org/10.1016/j.isci.2020.101893

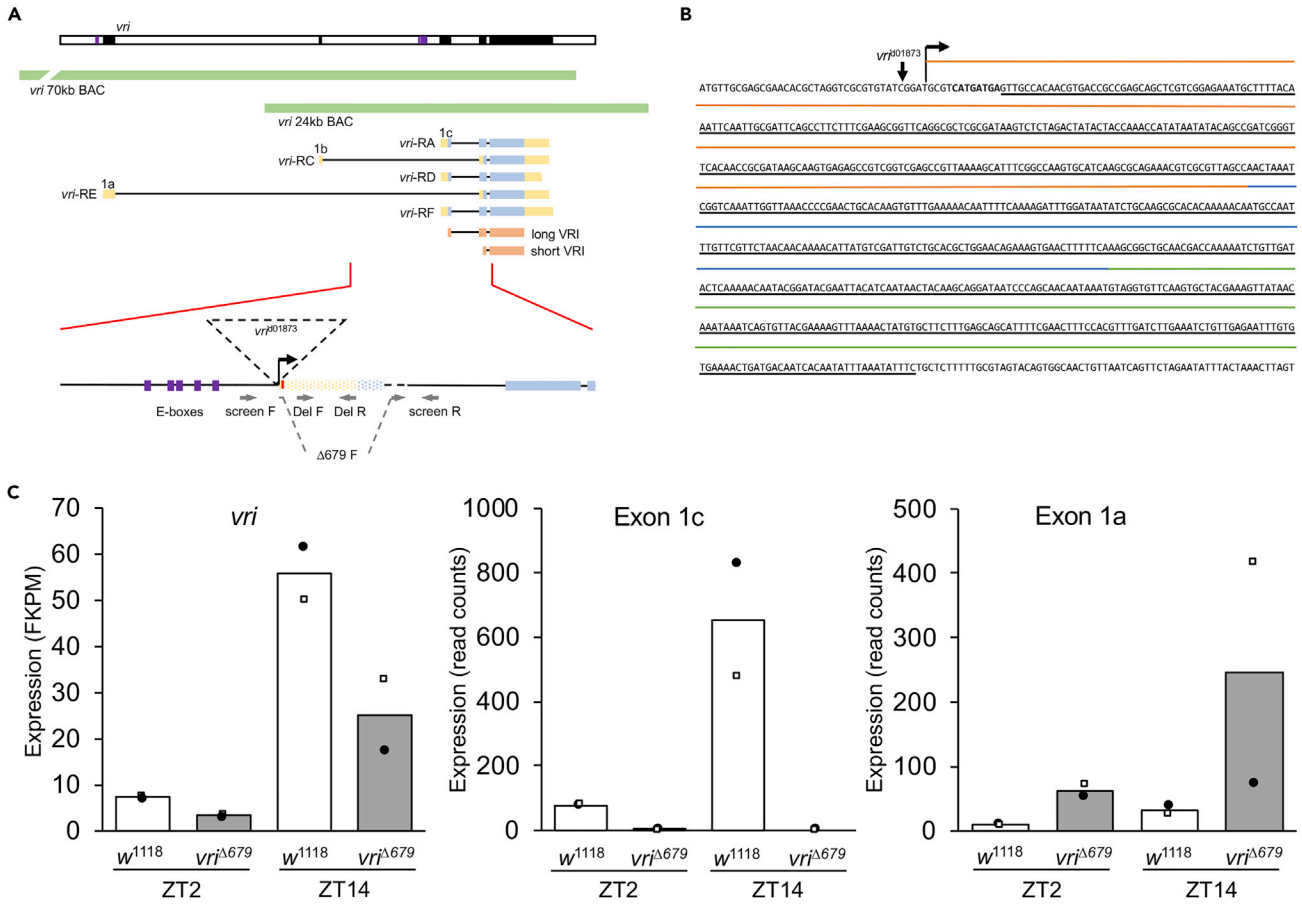

Figure 1. *vri*$^{\Delta 679}$ mutants lack *vri*-ADF transcript expression

(A) The *vri* genomic region (white box) showing *vri* exons (black boxes) and canonical E-box regulatory elements (purple lines) is depicted above the *vri* 70-kb BAC and *vri* 24-kb BAC transgenes (green boxes) that were used to rescue developmental and circadian function in *vri* mutants (see Figures 4 and 5). The five *vri* mRNA isoforms (RA, RC, RD, RE, RF) and the three alternate first exons (1a, 1b, 1c) are shown, where exons for different *vri* transcripts are shown as boxes denoting untranslated (yellow) or translated (blue) regions. The five *vri* transcripts produce short VRI or long VRI isoforms, depicted by orange boxes corresponding to their exon coding sequences. A magnified view of the *vri* genomic region bracketed by the red lines is shown below the short VRI and long VRI isoforms. Canonical E-box regulatory elements (purple boxes) are shown upstream of the *vri*^{d01873} P element (dashed triangle), which is located 4 bp upstream of exon 1c. Imprecise excision of *vri*^{d01873} produced a deletion removing most of exon 1 (stippled yellow and blue region) and a part of intron 1 (dashed line) and inserted an 8-bp sequence (red). The location and orientation (gray arrows) of the screen forward (screen F), screen reverse (screen R), Δ679 forward (Δ679 F), Deletion forward (Del F), and Deletion reverse (Del R) primers used to identify and characterize *vri* deletions are denoted.

(B) Sequence of the *vri* exon 1c region showing the *vri*^{d01873} P element insertion site, the *vri*$^{\Delta 679}$ deletion (underlined nucleotides), the 5′ untranslated region (orange line), the translated region (blue line), intron 1 (green line), and the 8-bp insertion (bold).

(C) RNA-seq analysis of *vri* expression in heads from *w*^{1118} and *vri*$^{\Delta 679}$ flies collected at ZT2 and ZT14 during LD cycles. The left graph shows composite mRNA expression levels in fragments per kilobase million (FPKM) for all *vri* mRNA isoforms (*vri*), the middle graph shows mRNA expression levels in read counts for exon 1c, and the right graph shows mRNA expression levels in read counts for exon 1a. Data from the two biological replicates are shown as black circles and white squares, and the average is shown by the bar height.

in embryos, pupae, and adults, and *vri*-ADF mRNA is present at all developmental stages (Thurmond et al., 2019). Rhythmic *vri* transcription is thought to be driven by CLK-CYCLE (CLK-CYC) binding to E-box regulatory elements upstream of exon 1c (Abruzzi et al., 2011; Blau and Young, 1999; Cyran et al., 2003; Lim et al., 2007). Based on these observations, we hypothesize that short VRI produced by *vri*-E is responsible for *vri* developmental functions and long VRI produced by *vri*-ADF mediates circadian function. If true, eliminating transcription from exon 1c should eliminate *vri* circadian function but leave *vri* developmental functions intact.

Here we generate a *vri* mutant (*vri*$^{\Delta 679}$) that eliminates *vri*-ADF mRNA production. This mutant is homozygous viable, demonstrating that *vri*-ADF mRNA is dispensable for fly development. Both *vri*-ADF and *vri*-E

Genotype	N	% Rhythmic	Period ±SEM	Strength ±SEM
w^{1118}	32	93.8±	23.77 ± 0.05[a]	310.08 ± 40.56
vri^{d01873}[b]	62	85.5±	23.30 ± 0.05	112.97 ± 11.59[c]
$vri^{\Delta 679}$[d]	63	93.5±	22.92 ± 0.05[e]	202.14 ± 16.94[f]
$vri^{\Delta 679}$; *vri* 24[g]	22	95.5±	23.29 ± 0.05	309.33 ± 38.59

Table 1. $vri^{\Delta 679}$ mutants show activity rhythms with a shorter period

[a]The period of w^{1118} activity rhythms is significantly longer ($p \leq 0.001$) than all other genotypes.
[b]Complete genotype is w^{1118}; vri^{d01873}; +.
[c]The power of vri^{d01873} flies is significantly lower ($p \leq 0.02$) than all other genotypes.
[d]Complete genotype is w^{1118}; *vri* $^{\Delta 679}$; +.
[e]The period of $vri^{\Delta 679}$ activity rhythms is significantly shorter ($p \leq 0.002$) than all other genotypes.
[f]The power of $vri^{\Delta 679}$ flies is significantly lower ($p \leq 0.02$) than w^{1118} and $vri^{\Delta 679}$; *vri* 24. N, total number of flies tested.
[g]Complete genotype is w^{1118}; *vri* $^{\Delta 679}$; *vri*24.

mRNAs are rhythmically expressed, but E-boxes situated near the *vri*-ADF promoter are required for viability, which suggests that they are important for *vri*-E transcription during development. Although *vri*-ADF mRNA and long VRI are absent in $vri^{\Delta 679}$ flies, low levels of cycling short VRI protein derived from *vri*-E mRNA are sufficient for behavioral rhythms. Surprisingly, *vri*-ADF mRNA primarily produces short VRI, likely due to the poor Kozak sequence context of the long VRI initiation codon relative to that of short VRI. These results suggest that short VRI carries out both developmental and circadian functions in *Drosophila*, where *vri*-E transcripts primarily support developmental function and *vri*-ADF transcripts primarily support circadian function.

RESULTS

A mutant that eliminates *vri*-ADF transcripts maintains clock function

As *vri*-ADF transcripts are thought to mediate clock function based on the clustering of E-boxes in their promoter, we sought to determine the significance of *vri*-ADF transcripts for clock function by generating a mutant that eliminates these transcripts. The vri^{d01873} P element is inserted 4 bp upstream of the exon 1c transcription start site (Figure 1A and 1B), is homozygous viable, and displays activity rhythms similar to those in w^{1118} wild-type controls (Table 1). The vri^{d01873} P element was excised (see Transparent Methods), and progeny lacking the vri^{d01873} insert were screened by PCR to identify flies carrying a deletion that disrupts exon 1c (Table S1 and Figure S1). The largest deletion mutant recovered, *vri* $^{\Delta 679}$, removes a 679-bp region that includes the last 513 nucleotides of exon 1c and 166 bp from intron 1 (Figures 1A, 1B, and S1). An 8-bp sequence was inserted within the deleted region (Figure 1B), possibly due to a P element local hop during the excision process (Tower et al., 1993). Although the transcription start site for exon 1c is intact in *vri* $^{\Delta 679}$ flies, the splice donor sequence for this exon is eliminated, thus any transcript initiated at exon 1c will be defective. RNA-seq analysis of control and *vri* $^{\Delta 679}$ flies collected when *vri* mRNA is lowest in wild-type flies at zeitgeber time 2 (ZT2, where ZT0 is lights on and ZT12 is lights off) and when *vri* mRNA is highest in wild-type flies at ZT14 during a 12 h light: 12 h dark (LD) cycle shows that transcript reads from exon 1c are almost entirely eliminated at both ZT2 and ZT14 in *vri* $^{\Delta 679}$ flies, whereas exon 1c transcript reads from control flies are >8-fold higher at ZT14 than at ZT2 as expected (Figure 1C; Table S1). This result indicates that the *vri* $^{\Delta 679}$ mutation essentially eliminates *vri*-ADF mRNA expression. In contrast, ~6-fold higher transcript reads were detected for exon 1a in $vri^{\Delta 679}$ flies than w^{1118} controls, where the number of reads was ~3-fold higher at ZT14 than ZT2 for each genotype (Figure 1C), which suggests that *vri*-E mRNA cycles in both w^{1118} and $vri^{\Delta 679}$ flies and is the predominant *vri* transcript in *vri* $^{\Delta 679}$ flies. Despite the loss of *vri*-ADF transcripts from exon 1c, *vri* $^{\Delta 679}$ mutant flies are homozygous viable, confirming that *vri*-ADF mRNAs are not necessary for development.

We expected $vri^{\Delta 679}$ flies to be behaviorally arrhythmic because they lack the *vri*-ADF mRNAs thought to be required for clock output (Gunawardhana and Hardin, 2017). Surprisingly, >93% of $vri^{\Delta 679}$ flies were rhythmic with an ~0.8 h shorter period than w^{1118} controls (Table 1). Given the quasi-normal $vri^{\Delta 679}$ behavioral rhythms, we assessed VRI expression in $vri^{\Delta 679}$ brains. VRI levels in all $vri^{\Delta 679}$ brain pacemaker neurons were sharply reduced compared with w^{1118} control brains (Figure 2A). Likewise, VRI levels were much lower in heads from $vri^{\Delta 679}$ flies than w^{1118} controls, but continued to cycle in abundance (Figure 2B). This result

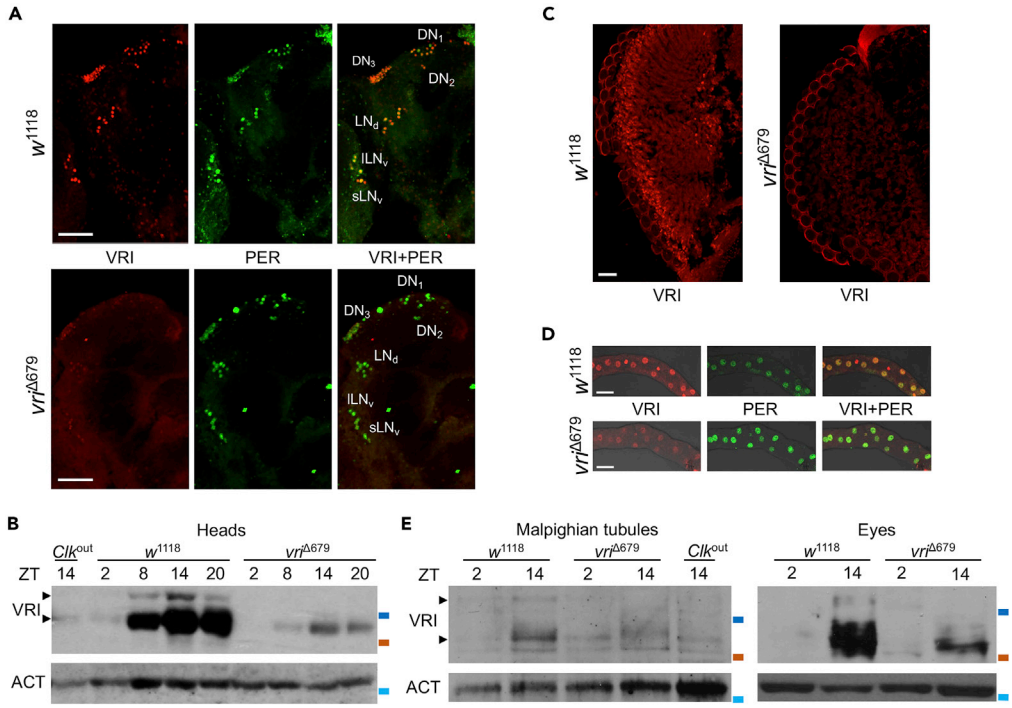

Figure 2. Low-level rhythms in VRI expression are observed in $vri^{\Delta 679}$ mutants

(A) Brains from control w^{1118} and $vri^{\Delta 679}$ flies were collected at ZT20 and were immunostained with VRI (red) and PER (green) antisera. Merged VRI + PER images are shown in yellow. The following brain pacemaker neuron groups were detected: dorsal neuron 1 (DN_1), dorsal neuron 2 (DN_2), dorsal neuron 3 (DN_3), dorsal lateral neuron (LN_d), large ventrolateral neuron (lLN_v), and small ventrolateral neuron (sLN_v). Scale bars, 50 μm.

(B) Proteins from the heads of w^{1118}, $vri^{\Delta 679}$, and Clk^{out} flies collected during LD at zeitgeber time (ZT) 2, 8, 14, and 20 were used to prepare western blots. Westerns probed with VRI antiserum showed rhythmically expressed high- and low-mobility VRI bands (arrowheads). β-Actin (ACT) was used as a loading control. Molecular weight marker positions to the right are 95 kDa (blue) and 72 kDa (orange) on the VRI blot and 37 kDa (light blue) on the ACT blot.

(C) Heads from w^{1118} and $vri^{\Delta 679}$ mutant flies collected at ZT20 were cryosectioned and immunostained with VRI antiserum. Images of compound eyes are shown, with VRI (red) staining detected in photoreceptor nuclei (white arrows). Scale bars, 20 μm.

(D) Malpighian tubules from w^{1118} and $vri^{\Delta 679}$ mutant flies collected at ZT20 were immunostained with VRI (red) and PER (green) antisera. Merged VRI + PER images are shown as yellow. Scale bars, 50 μm.

(E) Proteins from Malpighian tubule tissue samples (left) and compound eyes (right) of w^{1118} and $vri^{\Delta 679}$ flies collected during LD at ZT2 and ZT14 were used to prepare western blots. Westerns probed with VRI antiserum showed rhythmically expressed high- and low-mobility VRI bands (arrowheads). β-Actin (ACT) was used as a loading control. Molecular weight marker positions to the right are 95 kDa (blue) and 72 kDa (orange) on the VRI blots and 37 kDa (light blue) on the ACT blots.

suggests that VRI expression in retinal photoreceptors, which comprise >80% of all clock cells in the head (Glossop et al., 2003), is also reduced in $vri^{\Delta 679}$ flies. Indeed, as in brain pacemaker neurons VRI levels are greatly reduced in photoreceptor cells (Figure 2C). Likewise, VRI levels were low in Malpighian tubules (MTs) (Figure 2D), a clock-containing tissue that mediates renal function in *Drosophila* (Dow and Romero, 2010). Although greatly reduced, VRI levels in photoreceptor cells and MTs of $vri^{\Delta 679}$ flies are rhythmically expressed (Figure 2E). Decreased levels of VRI in $vri^{\Delta 679}$ flies likely shorten circadian period by increasing *Clk* expression because VRI acts to repress *Clk* transcription and increased *Clk* expression shortens circadian period (Allada et al., 2003; Cyran et al., 2003; Glossop et al., 2003). Consistent with this possibility, *Clk* mRNA is ~50% higher on average in $vri^{\Delta 679}$ flies than w^{1118} controls (Figure S2). In addition, CLK-CYC targets *per* and *tim* are also upregulated in $vri^{\Delta 679}$ flies, but *cyc*, which is not regulated by the circadian clock (Liu et al., 2017; Nagoshi et al., 2010), is expressed at about the same levels in $vri^{\Delta 679}$ and w^{1118} flies (Figure S2). These results show that *vri*-ADF expression is not required for rhythmic behavior *per se*, although the lower levels of VRI in $vri^{\Delta 679}$ flies likely shorten circadian period through their impact on *Clk* expression.

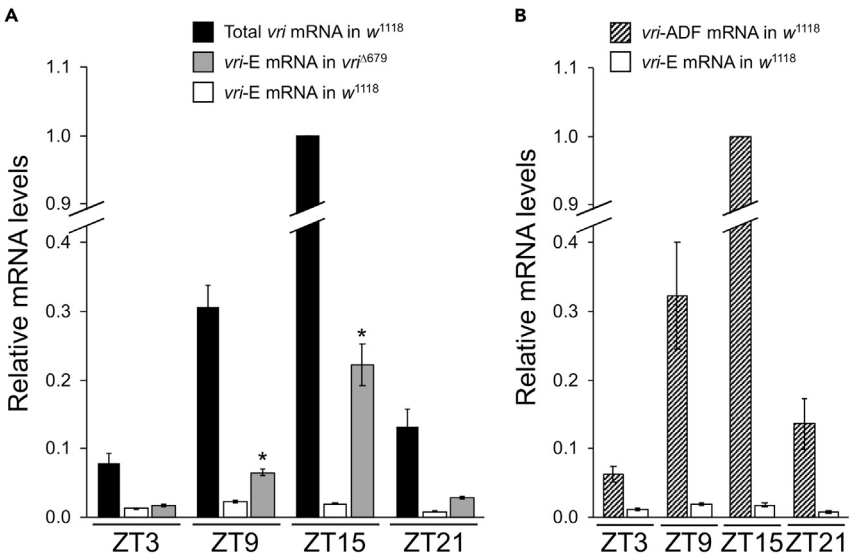

Figure 3. *vri*-E mRNA cycling and upregulation in $vri^{\Delta 679}$ flies

(A) RT-qPCR quantification of total *vri* mRNA levels in heads of w^{1118} flies (black bar), *vri*-E mRNA levels in heads of $vri^{\Delta 679}$ flies (gray bars), and *vri*-E mRNA levels in heads of w^{1118} flies (white bar) collected at the indicated times during LD. Levels of *vri*-E mRNA are relative to the total *vri* mRNA level at ZT15 in w^{1118} flies, which was set to 1.0. * Abundance of *vri*-E mRNA is significantly ($p \leq 0.0002$) lower than total *vri* mRNA based on Student's two-tailed t test.

(B) RT-qPCR quantification of *vri*-ADF (hatched bar) and *vri*-E (white bar) mRNA levels in heads of w^{1118} flies collected at the indicated times during LD. Levels of *vri*-ADF and *vri*-E mRNAs are relative to the *vri*-ADF mRNA peak at ZT15, which was set to 1.0.

As *vri*-ADF expression is virtually eliminated in $vri^{\Delta 679}$ adults, *vri*-E expression presumably accounts for the cycling VRI levels and rhythmic behavior in $vri^{\Delta 679}$ flies. Indeed, RNA-seq analysis shows that *vri*-E expression, as reflected by exon 1a transcription, is even higher in $vri^{\Delta 679}$ flies than w^{1118} controls, but continues to have higher expression levels at ZT14 than ZT2 like control w^{1118} flies (Figure 1C). These results suggest that *vri*-E mRNA is upregulated in $vri^{\Delta 679}$ flies and cycles in abundance. To confirm *vri*-E mRNA upregulation and cycling in $vri^{\Delta 679}$ flies, RT-qPCR was carried out on head RNA from control w^{1118} and in $vri^{\Delta 679}$ flies collected every 6 h during LD. Total *vri* mRNA, *vri*-ADF mRNA, and *vri*-E mRNA in wild-type flies and *vri*-E mRNA in $vri^{\Delta 679}$ flies all showed significant ($p \leq 0.006$) rhythmicity by one-way ANOVA (see Transparent Methods). When the levels of *vri*-E in w^{1118} and $vri^{\Delta 679}$ flies are plotted relative to total *vri* mRNA in w^{1118} flies, *vri*-E mRNA levels are >10-fold higher in $vri^{\Delta 679}$ than w^{1118} flies at ZT15, when *vri*-E peaks in $vri^{\Delta 679}$ flies, and are almost 3-fold higher at ZT9, when *vri*-E peaks in w^{1118} flies (Figure 3A). Thus, the loss of exon 1c results in higher levels of *vri*-E mRNA with a delayed ZT15 peak, which is the same peak phase as the major *vri*-ADF transcript in w^{1118} flies (Figures 3B and 1C). This shift in *vri*-E expression in $vri^{\Delta 679}$ flies suggests that the level and phase of rhythmic *vri* expression is in part compensated in the absence of exon 1c. Importantly, given that $vri^{\Delta 679}$ flies only express *vri*-E mRNA, *vri*-E is sufficient for both fly development and circadian behavioral rhythms.

E-boxes located upstream of *vri* exon 1c are essential for development

CLK-CYC binding to E-box regulatory elements having the canonical sequence CACGTG drives rhythmic transcription (Darlington et al., 1998; Yu and Hardin, 2006). Five canonical E-boxes are situated within 2.5 kb upstream of *vri* exon 1c (Figure 4). These E-boxes are centered on the strongest CLK-CYC binding site in the *Drosophila* genome (Abruzzi et al., 2011) and likely account for high levels of rhythmic *vri* transcription (Blau and Young, 1999). In addition, two canonical E-boxes <1.5 kb upstream of exon 1a are located within another strong CLK-CYC binding site (Abruzzi et al., 2011) and likely contribute to rhythmic expression of *vri*-E mRNA.

Previously we demonstrated that a ~70-kb BAC clone (CH321-28 × 10^{21}), which covers the *vri* genomic region (Figure 1A), rescues molecular and behavioral rhythms in vri^{5} null mutant flies (Gunawardhana and Hardin, 2017). To test whether E-boxes in the exon 1c promoter are necessary for high levels of rhythmic *vri*

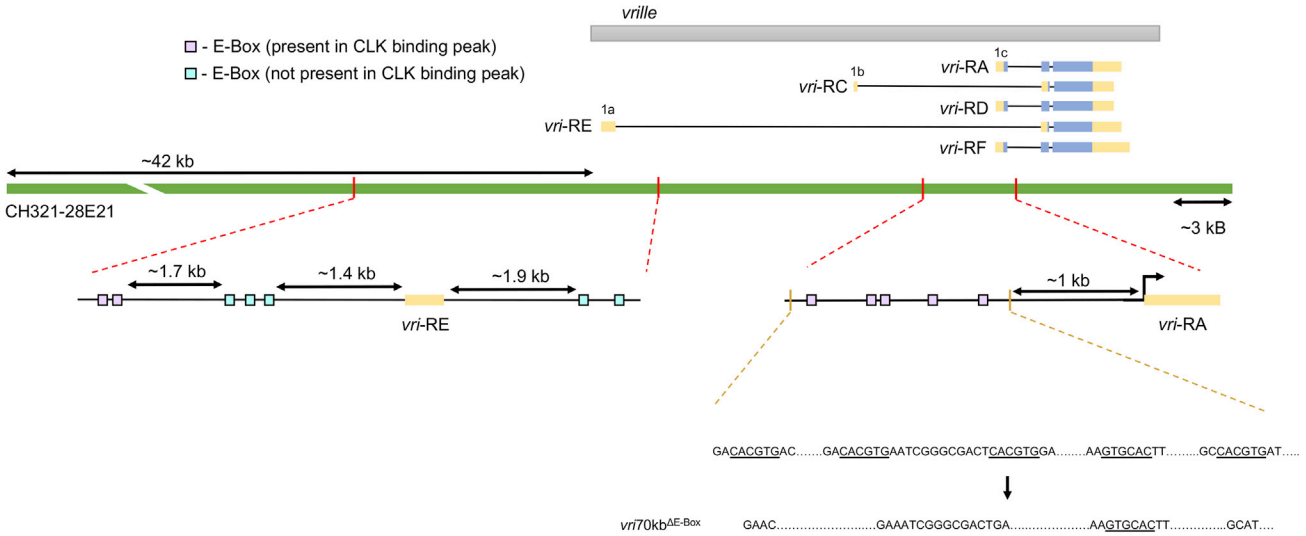

Figure 4. Diagram of *vri*70kb$^{\Delta E-Box}$ transgene

A ~70-kb BAC clone (CH321-28 × 10[21]), which is ~42 kb upstream and ~3 kb downstream of the *vri* gene, was used to generate the *vri*70kb$^{\Delta E-Box}$ transgene. Multiple E-box regulatory sequences are found nearby *vri* exons 1a and 1c (expanded diagram with red dashed lines) which are found within CLK binding peaks (aqua boxes) or outside CLK binding peaks (purple boxes). Four of the five E-boxes within 2.5 kb upstream of exon 1c were deleted (expanded diagram with brown dashed lines) to generate the *vri*70kb$^{\Delta E-Box}$ mutant transgene containing one intact E-box.

transcription, four of the five E-boxes upstream of exon 1c were deleted in this BAC clone via site-directed mutagenesis (Figure 4). The resulting *vri*70kb$^{\Delta E-Box}$ mutant was integrated into three independent docking sites (VK5, VK13, and VK20) on chromosome 3 using *PhiC32*-mediated recombination (Venken et al., 2006). Surprisingly, none of the *vri*70kb$^{\Delta E-Box}$ transgenic lines rescued the developmental lethality in the *vri*^{5} null mutant, which suggests that these E-boxes are essential for development. As we cannot distinguish between *vri* mRNA and protein produced by endogenous *vri* and the *vri*70kb$^{\Delta E-Box}$ transgene, we could not determine whether the *vri*70kb$^{\Delta E-Box}$ transgene was expressed in the presence of wild-type *vri*. Thus, even though *vri*-E transcripts are sufficient for development in *vri* $^{\Delta 679}$ flies, the regulatory elements that remain in the *vri*70kb$^{\Delta E-Box}$ transgene are incapable of driving sufficient *vri* expression during development to rescue lethality of the *vri*^{5} mutant.

vri-ADF mRNA primarily produces the short VRI isoform

To restore *vri*-ADF mRNA and long VRI protein expression in *vri*$^{\Delta 679}$ flies, a ~24-kb BAC clone (CH322-102O15) was used to generate the *vri*24 transgene (Figure 5A). This transgene was unable to rescue developmental lethality of the *vri*^{5} null mutant, suggesting that *vri*-ADF mRNA is not sufficient for fly development. However, *vri*24 rescued wild-type levels of VRI expression in *vri*$^{\Delta 679}$ brain pacemaker neurons and fly heads, where VRI in fly heads cycled with low levels at ZT2 and high levels at ZT14 (Figures 5B and 5C). Moreover, the *vri*24 transgene partially rescues the short period (~22.9 h) activity rhythms of *vri*$^{\Delta 679}$ flies by lengthening period to ~23.3 h (Table 1). Thus, *vri*-ADF mRNA driven by *vri*24 supplements the low VRI levels derived from *vri*-E mRNA, thereby lengthening the short circadian period of *vri*$^{\Delta 679}$ flies.

Although *vri*-E is the only *vri* transcript present in *vri*$^{\Delta 679}$ flies (Figure 1C), VRI from *vri*$^{\Delta 679}$ flies co-migrates with the major VRI band from control w^{1118} flies (Figure 2), which is surprising because *vri*-E mRNA encodes short VRI and the much more abundant *vri*-ADF mRNA encodes long VRI (Figures 1C and 3B). To unequivocally identify the VRI isoform produced by *vri*-ADF mRNA, a 5.3-kDa V5-3xHA epitope tag was added to the *vri*24 transgene at the N terminus of long VRI. Western blots containing proteins from the heads of w^{1118} flies containing *vri*24HA and w^{1118} control flies were collected at ZT14 and probed with VRI and hemagglutinin (HA) antibodies. Surprisingly, no VRI band could be detected from the *vri*24HA strain with HA antibody (Figure S3). If the weak >90-kDa VRI band seen in w^{1118} flies corresponds to long VRI (Figures 2B and 2E), then the V5-3xHA-tagged long VRI band may not be expressed at high enough levels to detect. To detect VRI from *vri*24HA flies with greater sensitivity, we immunoprecipitated 10-fold more head extract from flies collected at ZT14 with VRI antibody. This immunoprecipitate, along with head extracts from *vri*24HA and

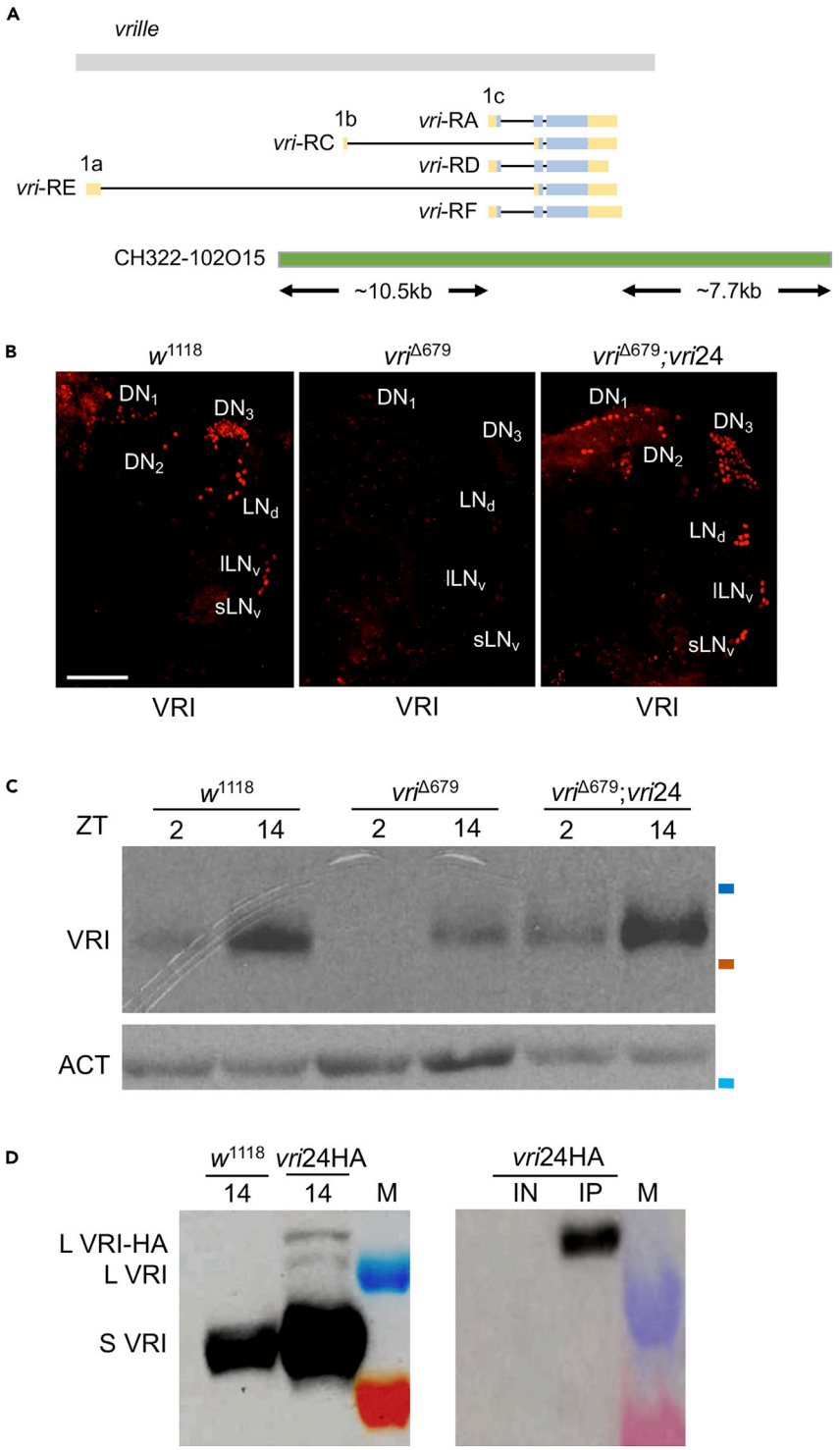

Figure 5. *vri*24kb transgene rescues *vri*$^{\Delta 679}$ mutant phenotypes

(A) Diagram depicting the ~24-kb BAC clone (CH322-102O15) that was used to generate the *vri*24 transgene (green rectangle), which produces a V5-3xHA epitope-tagged VRI protein. This BAC clone is ~10.5 kb upstream of the *vri*-ADF mRNA transcription start site and ~7.7 kb downstream of *vri*-ADF mRNAs.

(B) Brains from wild-type (w^{1118}), *vri*$^{\Delta 679}$ mutants, and *vri*$^{\Delta 679}$; *vri*24 flies were collected at ZT19 and were immunostained with VRI antisera. The following brain pacemaker neuron groups were detected: dorsal neuron 1 (DN_1), dorsal neuron 2 (DN_2), dorsal neuron 3 (DN_3), dorsal lateral neuron (LN_d), large ventrolateral neuron (lLN_v), and small ventrolateral neuron (sLN_v). Scale bar, 50 μm.

Figure 5. *Continued*

(C) Protein from the heads of w^{1118}, $vri^{\Delta 679}$ mutants and $vri^{\Delta 679}$; *vri*24 flies collected during LD at the specified times were used to generate western blots that were probed with VRI antiserum. β-Actin (ACT) was used as a loading control. Molecular weight marker positions to the right of the blot are 95 kDa (blue) and 72 kDa (orange) on the VRI blot and 37 kDa (light blue) on the ACT blot.

(D) Protein from the heads of w^{1118} flies containing *vri*24HA and w^{1118} control flies collected at ZT14 were used to generate western blots that were probed with VRI antiserum (left). Protein from the heads of w^{1118} flies containing *vri*24HA collected at ZT14 was run directly as input (IN) or as an immunoprecipitate (IP) using VRI antibody on western blots that were probed with HA antiserum (right). Long-VRI, short-VRI, and VRI-HA bands are detected next to the 95 kD (blue) and 72 kD (red) protein markers.

w^{1118} flies collected at ZT14, were used to prepare western blots that were probed with VRI and HA antibodies. VRI antibody detected three bands in *vri*24HA flies: a major band running at ~85 kDa, a minor band running at >90 kDa, and a minor band running at >95 kDa (Figure 5D). Based on gel migration, the >95 kDa band corresponds to V5-3xHA-tagged long VRI that is also detected with HA antibody, the >90-kDa band corresponds to the long VRI band in w^{1118} flies, and the ~85-kDa band corresponds to the prominent VRI band (short VRI) in w^{1118} flies (Figure 5D). These results demonstrate that long VRI is expressed at low levels compared with short VRI and suggests that *vri*-ADF mRNA primarily produces short VRI rather than long VRI.

AUG context accounts for preferential production of short VRI by *vri*-ADF mRNA

To confirm that mRNA encoding long VRI also produces short VRI, cDNAs encoding C-terminal FLAG-HA epitope-tagged long VRI (*vri*A) or short VRI (*vri*C) were expressed in S2 cells. As expected, S2 cells expressing *vri*C showed only a short VRI band, whereas S2 cells expressing *vri*A showed weak long VRI and strong short VRI bands (Figure 6A). The VRI bands expressed by *vri*A and *vri*C in S2 cells ran at a higher mobility than their corresponding VRI bands in fly heads due to the 4.8-kDa epitope tag (Figure 6A). To demonstrate that mRNAs encoding long VRI can produce short VRI *in vivo*, *tim*(UAS)Gal4 was used to drive a UAS-*vri* cDNA encoding long VRI and *tim*-Gal4 was used to overexpress endogenous *vri*-ADF mRNA via a UAS element in the vri^{d01873} P{XP} transposon inserted 4 bp upstream of *vri* exon 1c (Thibault et al., 2004). Although both long and short VRI isoforms were produced by *tim*(UAS)-Gal4 driven UAS-*vri* and *tim*-Gal4-driven vri^{d01873}, short VRI was the predominant isoform produced (Figure 6B).

Generally, translation initiation is most efficient when the start codon resides within a strong Kozak sequence, which is optimally GCCGCC[A|G]CC**AUG**G in *Drosophila* (Feng et al., 1991). We determined the Kozak sequence for the long VRI and short VRI start codons and found that the short VRI start codon has an 8/13 identity with the optimal *Drosophila* Kozak sequence versus the long VRI start codon, which had a 5/13 identity (Figure 6C). Moreover, a uracil at the −3, −2, −1, and +4 positions with respect to the translation initiation site weakens translation initiation (Feng et al., 1991). The long VRI start codon had uracil at three of four of these positions, whereas the short VRI start codon had no uracils in these positions (Figure 6C). These data suggest that the short VRI start codon possesses a strong Kozak sequence that more efficiently initiates translation.

DISCUSSION

Previous work demonstrated that *vri* regulates developmental and clock-controlled processes in *Drosophila* (Blau and Young, 1999; George and Terracol, 1997; Gunawardhana and Hardin, 2017). The *vri* gene produces multiple transcripts and two proteins during development and in adults (Blau and Young, 1999; George and Terracol, 1997; Glossop et al., 2003), but the extent to which each transcript and protein isoform contributes to developmental and clock functions is not known. The $vri^{\Delta 679}$ mutant generated here specifically eliminates *vri*-ADF mRNA expression (Figure 1C), which shortens the period of activity rhythms (Table 1). As VRI represses *Clk* transcription (Cyran et al., 2003; Glossop et al., 2003), the low levels of *vri* expression in $vri^{\Delta 679}$ flies likely shorten period by increasing *Clk* levels (Figure S2), consistent with previous results (Zhao et al., 2003). As $vri^{\Delta 679}$ flies are homozygous viable, the only remaining *vri* mRNA expressed, *vri*-E, is sufficient to rescue *vri* developmental and clock function (Figures 1C, 2, and S1).

Although *vri*-E mRNA expression is much lower than *vri*-ADF in wild-type flies (Figures 1C and 3D), *vri*-E is rhythmically expressed (Figure 3). There is a strong CLK-CYC binding site containing two canonical E-boxes

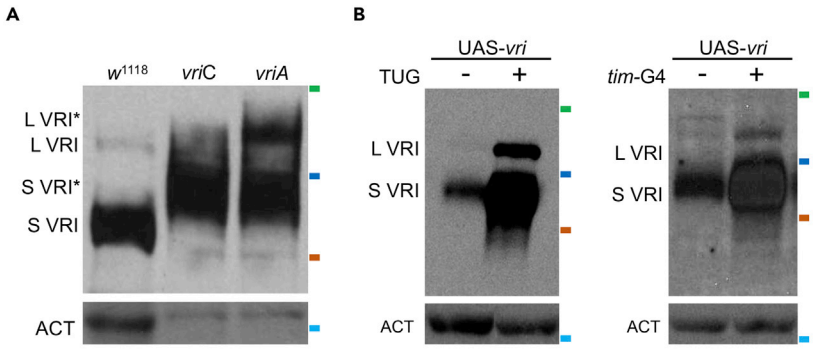

C

	-9	-8	-7	-6	-5	-4	-3	-2	-1	+1	+2	+3	+4	
Optimal Kozak sequence	G	C	C	G	C	C	A/G	C	C	**A**	**U**	**G**	G	
First VRI start codon	C	A	A	A	A	C	A	U	U	A	U	G	U	
	-	-	-	-	-	*	*	-	-	*	*	*	-	5/13
Second VRI start codon	U	C	C	A	C	A	G	C	A	A	U	G	C	
	-	*	*	-	*	-	*	*	-	*	*	*	-	8/13

Figure 6. *vri*-ADF mRNAs generate short protein using an alternative translation initiation site

(A) Western blot of proteins from heads of w^{1118} flies collected at ZT15 and S2 cells overexpressing *vri*C and *vri*A transcripts were probed with VRI antiserum. β-Actin (ACT) was used as a loading control. Long VRI, L-VRI; Long VRI-FLAG-HA, L-VRI*; Short VRI, S-VRI; Short VRI-FLAG-HA, S-VRI*. Molecular weight marker positions to the right are 130 kDa (green), 95 kDa (blue), and 72 kDa (orange) on the VRI blot and 37 kDa (light blue) on the ACT blot.

(B) Western blots of proteins from heads of flies collected at ZT15 that contain (left) UAS-*vri* only (–) and UAS-*vri* driven by *tim*-(UAS)-Gal4 (+) or (right) vri^{d01873} only (–) and vri^{d01873} driven by *tim*-Gal4 (+) were probed with VRI antiserum. Loading control and abbreviations are as described in (A). Molecular weight markers to the right are 130 kDa (green), 95 kDa (blue), and 72 kDa (orange) on the VRI blot and 37 kDa (light blue) on the ACT blot.

(C) Sequence comparison of Kozak sequences associated with the long VRI translation initiation codon (first VRI start codon) and the short VRI translation initiation codon (second VRI start codon) to the optimal Kozak sequence for *Drosophila melanogaster*. An asterisk (*) indicates a match, a dash (–) indicates a difference, and the number of matches of the 13 residues is noted at end of the row. The numbering on top represents the location of each base with respect to the first base of the translation initiation codon (+1).

~2.5 kb upstream of exon 1a (Abruzzi et al., 2011), which may account for *vri*-E mRNA cycling. The five canonical E-boxes present within 2.5 kb upstream of exon 1c coincide with the strongest CLK-CYC binding site in the *Drosophila* genome (Abruzzi et al., 2011) and presumably account for high-amplitude rhythms in *vri*-ADF mRNA levels. When we tested whether the $vri^{\Delta E\text{-box}}$ transgene, which removes four of five canonical E-boxes upstream of exon 1c (Figure 4), eliminates *vri*-ADF mRNA cycling, we were surprised to find that vri^{5} mutants containing the $vri^{\Delta E\text{-box}}$ transgene were not viable. This result suggests that E-boxes upstream of exon 1c are required for developmental expression of *vri*-E mRNA, which is sufficient to rescue developmental lethality. Notably, additional bHLH transcription factors such as MYC-MAX heterodimers bind CACGTG E-boxes in *Drosophila* (Gallant et al., 1996). We speculate that during development one or more bHLH transcription factors bind E-boxes upstream of exon 1c (intron 1 of the *vri*-E transcription unit) to promote transcription activation from exon 1a.

The long VRI and short VRI isoforms are encoded by the *vri*-ADF and *vri*-E transcripts, respectively (Gramates et al., 2017), but identifying short and long VRI bands on western blots has been a challenge because both VRI bands migrate much more slowly than the predicted short and long VRI molecular weights and the major VRI band in adults is the faster migrating band even though long VRI should be produced by abundant *vri*-ADF mRNA (Cyran et al., 2003; Glossop et al., 2003; Gunawardhana and Hardin, 2017). The *vri*24 transgene, which rescues $vri^{\Delta 679}$ period shortening and restores high levels of rhythmic VRI (Figure 5), was modified to epitope tag long VRI with V5-3xHA at the N terminus. Based on gel migration, the HA-

tagged long VRI band corresponds to the slow-migrating VRI band that runs at >90 kDa, and we infer that the faster migrating band that runs at ~85 kDa is short VRI.

Both long and short VRI are produced by cDNAs or genomic DNA that encodes only long VRI (Figure 6). As short VRI is produced using an in-frame AUG codon 119 amino acids downstream of the first AUG that initiates long VRI, we reasoned that the ribosome may not interact with the long VRI AUG as efficiently as the short VRI AUG. Indeed, the consensus Kozak sequence at the long VRI AUG is much weaker than that at the short VRI AUG. Although this difference in Kozak sequence strength may account for the relative expression levels of long and short VRI, other mechanisms could account for this difference. For instance, IRES sequences may direct the ribosome primarily to the short VRI AUG. In fact, the mammalian VRI ortholog, NFIL3/E4BP4, contains an IRES in its 5′ UTR that directs cap-independent translation (Kim et al., 2017). Whether such a mechanism functions to promote short VRI translation awaits further analysis. In any case, our analysis shows that short VRI is the predominant VRI isoform during development and in adults, which implies that short VRI mediates *vri* developmental and circadian function.

Limitations of the study

Although we show that *vri*-E mRNA is sufficient for activity rhythms, *vri*-E mRNA and short VRI are both rhythmically expressed at lower levels, thus providing no new insight into whether VRI cycling is dependent on *vri* mRNA cycling or whether rhythmic behavior is dependent on VRI rhythms. E-boxes upstream of the *vri*-ADF transcription start site are necessary for viability, but these results do not reveal the developmental processes, tissue(s), or transcription factors involved. Our results imply that short VRI is expressed from long VRI transcripts due to a weak Kozak consensus, but additional experiments such as swapping Kozak consensus sequences for long and short VRI are needed to confirm this conclusion.

Resource availability

Lead contact

Further information and requests for resources and reagents not made available through national stock centers should be directed to and will be fulfilled by the lead contact, Paul Hardin (phardin@bio.tamu.edu).

Materials availability

All unique/stable reagents generated in this study will be made available on request by the Lead Contact.

Data and code availability

The RNA-seq datasets generated during this study are available at the Gene Expression Omnibus Repository and can be accessed under the accession number GSE154785 (https://www.ncbi.nlm.nih.gov/geo/query/acc.cgi?acc=GSE154785).

METHODS

All methods can be found in the accompanying Transparent methods supplemental file.

SUPPLEMENTAL INFORMATION

Supplemental information can be found online at https://doi.org/10.1016/j.isci.2020.101893.

ACKNOWLEDGMENTS

We thank Joshua Meehan for assistance in conducting S2 cell culture experiments, Aldrin Lugena for assistance with RNA-seq analysis, and Michael Rosbash for providing anti-PER antibody. This work was supported by endowment funds from the John W. Lyons Jr. '59 Chair.

AUTHOR CONTRIBUTIONS

Conceptualization, P.E.H. and K.L.G.; Methodology, K.L.G. and G.B.S.R.; Investigation, K.L.G., C.C., and G.B.S.R.; Formal Analysis, K.L.G. and G.B.S.R.; Writing – Original Draft, K.L.G.; Writing – Review & Editing, P.E.H., K.L.G., C.C., and G.B.S.R.; Funding Acquisition and Supervision, P.E.H.

DECLARATION OF INTERESTS

The authors declare no competing interests.

Received: July 29, 2020
Revised: October 19, 2020
Accepted: December 2, 2020
Published: January 22, 2021

REFERENCES

Abruzzi, K.C., Rodriguez, J., Menet, J.S., Desrochers, J., Zadina, A., Luo, W., Tkachev, S., and Rosbash, M. (2011). Drosophila CLOCK target gene characterization: implications for circadian tissue-specific gene expression. Genes Dev. *25*, 2374–2386.

Allada, R., Kadener, S., Nandakumar, N., and Rosbash, M. (2003). A recessive mutant of Drosophila Clock reveals a role in circadian rhythm amplitude. EMBO J. *22*, 3367–3375.

Blau, J., and Young, M.W. (1999). Cycling *vrille* expression is required for a functional *Drosophila* clock. Cell *99*, 661–671.

Cyran, S.A., Buchsbaum, A.M., Reddy, K.L., Lin, M.C., Glossop, N.R., Hardin, P.E., Young, M.W., Storti, R.V., and Blau, J. (2003). *vrille, Pdp1*, and *dClock* form a second feedback loop in the *Drosophila* circadian clock. Cell *112*, 329–341.

Darlington, T.K., Wager-Smith, K., Ceriani, M.F., Staknis, D., Gekakis, N., Steeves, T.D., Weitz, C.J., Takahashi, J.S., and KAY, S.A. (1998). Closing the circadian loop: CLOCK-induced transcription of its own inhibitors *per* and *tim*. Science *280*, 1599–1603.

Dow, J.A., and Romero, M.F. (2010). Drosophila provides rapid modeling of renal development, function, and disease. Am. J. Physiol. Ren. Physiol *299*, F1237–F1244.

Feng, Y., Gunter, L.E., Organ, E.L., and Cavener, D.R. (1991). Translation initiation in Drosophila melanogaster is reduced by mutations upstream of the AUG initiator codon. Mol. Cell Biol. *11*, 2149–2153.

Gallant, P., Shiio, Y., Cheng, P.F., Parkhurst, S.M., and Eisenman, R.N. (1996). Myc and max homologs in Drosophila. Science *274*, 1523–1527.

George, H., and Terracol, R. (1997). The *vrille* gene of *Drosophila* is a maternal enhancer of *decapentaplegic* and encodes a new member of the bZIP family of transcription factors. Genetics *146*, 1345–1363.

Glossop, N.R., Houl, J.H., Zheng, H., Ng, F.S., Dudek, S.M., and Hardin, P.E. (2003). VRILLE feeds back to control circadian transcription of *Clock* in the *Drosophila* circadian oscillator. Neuron *37*, 249–261.

Gramates, L.S., Marygold, S.J., Santos, G.D., Urbano, J.M., Antonazzo, G., Matthews, B.B., Rey, A.J., Tabone, C.J., Crosby, M.A., Emmert, D.B., et al. (2017). FlyBase at 25: looking to the future. Nucleic Acids Res. *45*, D663–D671.

Gunawardhana, K.L., and Hardin, P.E. (2017). VRILLE controls PDF neuropeptide accumulation and arborization rhythms in small ventrolateral neurons to drive rhythmic behavior in Drosophila. Curr. Biol. *27*, 3442–3453.e4.

Hardin, P.E. (2011). Molecular genetic analysis of circadian timekeeping in Drosophila. Adv. Genet. *74*, 141–173.

Kim, H.J., Lee, H.R., Seo, J.Y., Ryu, H.G., Lee, K.H., Kim, D.Y., and Kim, K.T. (2017). Heterogeneous nuclear ribonucleoprotein A1 regulates rhythmic synthesis of mouse Nfil3 protein via IRES-mediated translation. Sci. Rep. *7*, 42882.

Lim, C., Chung, B.Y., Pitman, J.L., Mcgill, J.J., Pradhan, S., Lee, J., Keegan, K.P., Choe, J., and Allada, R. (2007). Clockwork orange encodes a transcriptional repressor important for circadian-clock amplitude in Drosophila. Curr. Biol. *17*, 1082–1089.

Liu, T., Mahesh, G., YU, W., and Hardin, P.E. (2017). CLOCK stabilizes CYCLE to initiate clock function in Drosophila. Proc. Natl. Acad. Sci. U S A *114*, 10972–10977.

Nagoshi, E., Sugino, K., Kula, E., Okazaki, E., Tachibana, T., Nelson, S., and Rosbash, M. (2010). Dissecting differential gene expression within the circadian neuronal circuit of Drosophila. Nat. Neurosci. *13*, 60–68.

Szuplewski, S., Kottler, B., and Terracol, R. (2003). The Drosophila bZIP transcription factor Vrille is involved in hair and cell growth. Development *130*, 3651–3662.

Thibault, S.T., Singer, M.A., Miyazaki, W.Y., Milash, B., Dompe, N.A., Singh, C.M., Buchholz, R., Demsky, M., Fawcett, R., Francis-Lang, H.L., et al. (2004). A complementary transposon tool kit for Drosophila melanogaster using P and piggyBac. Nat. Genet. *36*, 283–287.

Thurmond, J., Goodman, J.L., Strelets, V.B., Attrill, H., Gramates, L.S., Marygold, S.J., Matthews, B.B., Millburn, G., Antonazzo, G., Trovisco, V., et al. (2019). FlyBase 2.0: the next generation. Nucleic Acids Res. *47*, D759–D765.

Tower, J., Karpen, G.H., Craig, N., and Spradling, A.C. (1993). Preferential transposition of Drosophila P elements to nearby chromosomal sites. Genetics *133*, 347–359.

Venken, K.J., He, Y., Hoskins, R.A., and Bellen, H.J. (2006). P[acman]: a BAC transgenic platform for targeted insertion of large DNA fragments in D. melanogaster. Science *314*, 1747–1751.

Yu, W., and Hardin, P.E. (2006). Circadian oscillators of Drosophila and mammals. J. Cell Sci. *119*, 4793–4795.

Zhao, J., Kilman, V.L., Keegan, K.P., Peng, Y., Emery, P., Rosbash, M., and Allada, R. (2003). *Drosophila* clock can generate ectopic circadian clocks. Cell *113*, 755–766.

iScience, Volume *24*

Supplemental Information

Crosstalk between *vrille* transcripts, proteins, and regulatory elements controlling circadian rhythms and development in *Drosophila*

Kushan L. Gunawardhana, Gustavo B.S. Rivas, Courtney Caster, and Paul E. Hardin

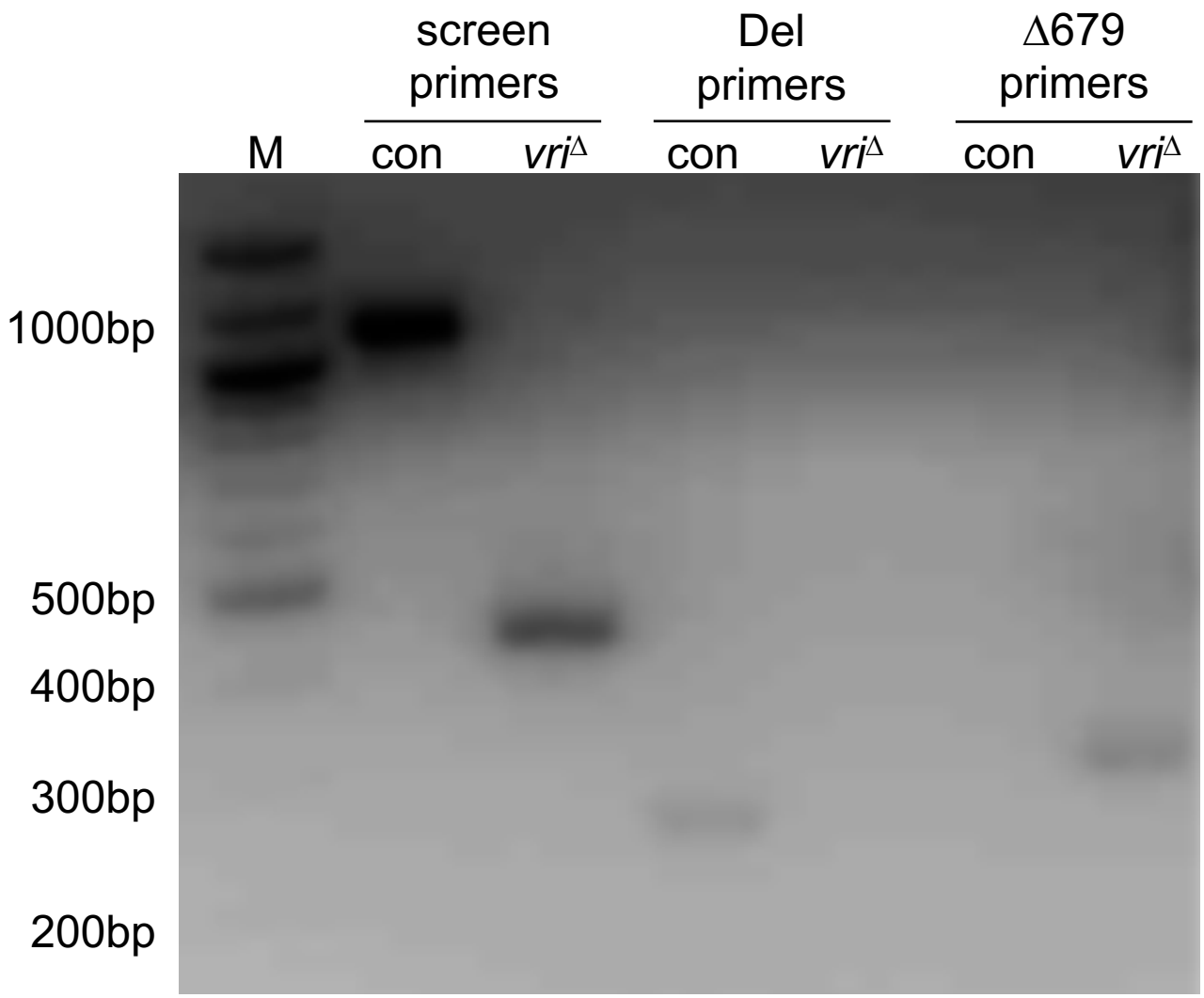

Figure S1. PCR amplification products from *w*^{1118} and *vri*$^{\Delta 679}$ genomic DNA. Related to Figure 1. Screen Forward and Screen Reverse primers produced an 1120bp band from *w*^{1118} DNA and a 411bp band from *vri*$^{\Delta 679}$ DNA, whereas Deletion Forward and Deletion Reverse primers (Del primers) produced a 267bp band from *w*^{1118} DNA, but no band from *vri*$^{\Delta 679}$ DNA. The Δ679 Forward primer contains the first 24bp of *vri*$^{\Delta 679}$ sequence from the *vri* transcription start consisting of the 4 remaining bases of the 5' UTR, an 8bp sequence insert (italics), and 12 bps from intron 1 (see panel A), and was used with Screen Reverse (Δ679 primers) to amplify a 275bp band from *vri*$^{\Delta 679}$ DNA, but no band from *w*^{1118} DNA.

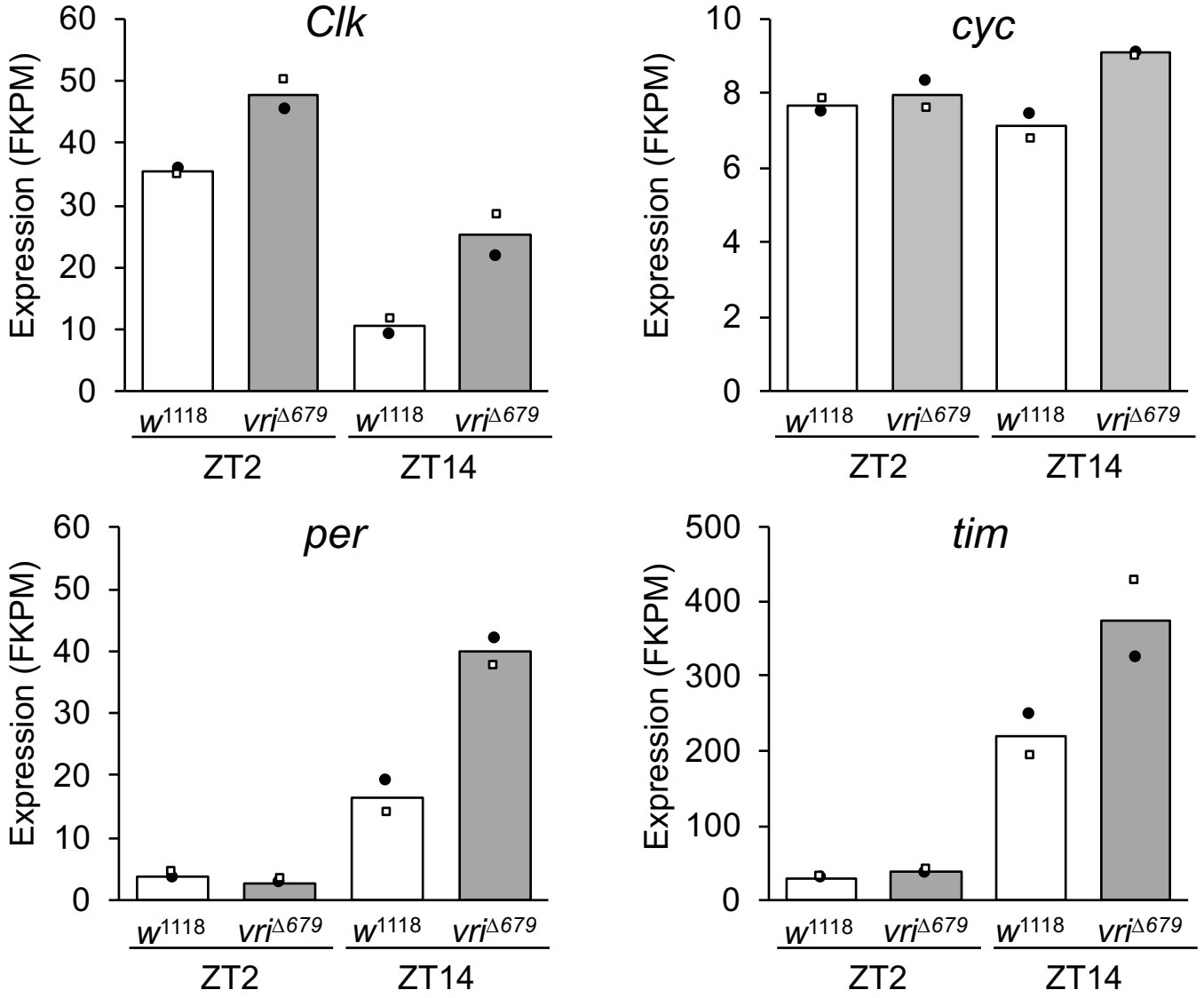

Figure S2. Clock gene expression in *vri*$^{\Delta 679}$ flies. Related to Figure 2. RNA-seq analysis of *Clk*, *cyc*, *per* and *tim* expression in heads from w^{1118} (white bars) and *vri*$^{\Delta 679}$ (gray bars) flies collected at ZT2 and ZT14 during LD cycles. Each graph shows mRNA expression levels in Fragments Per Kilobase Million (FPKM). Data from the two biological replicates are shown as black circles and white squares, and the average is shown by the bar height.

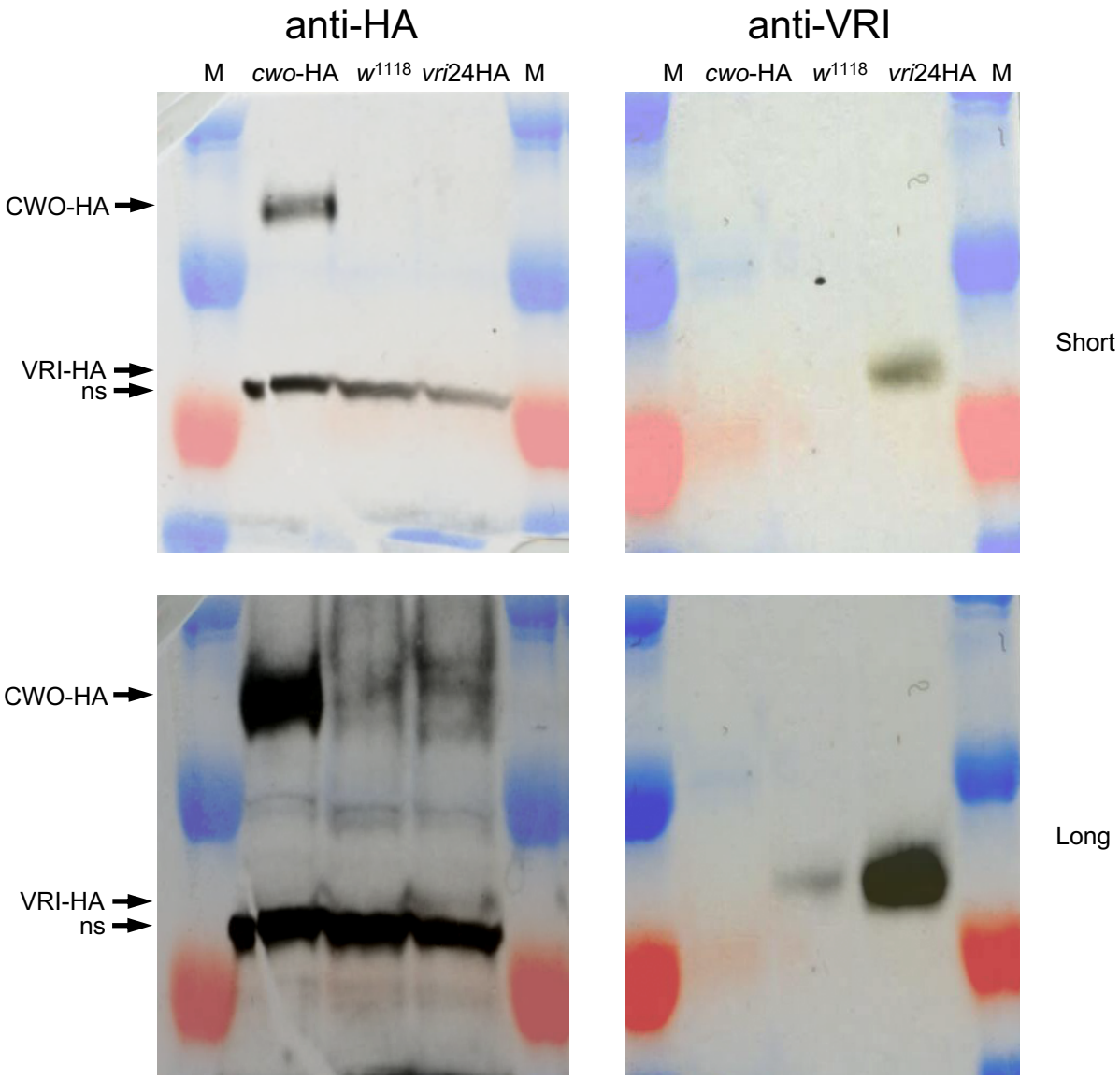

Figure S3. VRI-HA is not detected on western blots by anti-HA antibody. Related to Figure 5. w^{1118}, *w*; *cwo*-HA; + (*cwo*-HA), and w; *vri*24HA; + (*vri*24HA) flies were entrained for 3 days in LD, collected at ZT16 and protein extracts were prepared from heads. Protein extracts were used to prepare western blots probed with anti-HA and anti-VRI antibodies. Short (top) and long (bottom) exposures of the blot are shown. Arrows point to the CWO-HA, VRI-HA and a non-specific (ns) HA cross-reacting protein bands. Molecular weight markers (M) are 130kDa (blue, top), 95kDa (blue, second), 72kDa (red, third) and 56kDa (blue, bottom).

Table S1. **Related to Figure 1.** RNA-seq analysis of transcript reads in *vri* exons from w^{1118} control and $vri^{\Delta 679}$ mutant flies.

	w^{1118}	w^{1118}	w^{1118}	w^{1118}	$vri^{\Delta 679}$	$vri^{\Delta 679}$	$vri^{\Delta 679}$	$vri^{\Delta 679}$
vri exon	ZT2_R1	ZT2_R2	ZT14_R1	ZT14_R2	ZT2_R1	ZT2_R2	ZT14_R1	ZT14_R2
exon1a	11	9	38	26	53	72	74	416
exon1c	75	78	829	477	1	0	0	0
exon2	152	164	1724	1076	73	70	134	481
exon3s	1815	1633	16210	11588	710	669	2811	7003

Biological replicates were collected as described above. Values for mRNA expression for *vri* exon1a, exon1c, exon2 and exon3s (the shortest *vri* exon3 variant) are presented as read counts.

Transparent Methods

Fly strains

The following fly strains were used in this study: w^{1118}, st[1] Blm[D2] Sb[1] P{ry[+t7.2]=Δ2-3}99B (*P*[*ry*+ Δ2-3]) (BDSC), *tim*-Gal4 (Emery et al., 1998)(Emery et al., 1998), *tim(UAS)Gal4* (Blau and Young, 1999), gl^{60j} (Moses et al., 1989), vri^{d01873} (BDSC), *cwo*-HA (Zhou, 2017) and UAS-*vri* (Blau and Young, 1999). Flies were reared on standard cornmeal/agar medium supplemented with yeast and kept in 12 h light/12 h dark (LD) cycles at 25°C

vri^{d01873} P-element mobilization and *vri*$^{\Delta 679}$ mutant generation

The vri^{d01873} insertional mutant line was initially backcrossed seven times to w^{1118} flies. Then vri^{d01873} flies were crossed to *P*[*ry*+ Δ2-3] flies containing the P-element transposase. Progeny of the cross that had white eyes were crossed to w^{1118}; *CyO*/*sco* flies. Once the chromosome that contained the P-element was homozygous, the genomic DNA was extracted from 5-6 flies and screened for a deletion with Screen Forward (5' CGGCAATGTGATCGCTTGCAAC 3') and Screen Reverse (5' CATGCACGTACACTTAAGCGCTC 3') primers (Figure S1). The largest deletion strain, $vri^{\Delta 679}$, was characterized via PCR using the Deletion Forward (5' GATCGGGTTCACAACCGC 3') and Deletion Reverse (5' GTTCACTTTCTGTTCCAGCGTG 3') primer pair and the Δ679 Forward (5' GCGTCATGATGATGCTCTTTTTGC 3') and Screen Reverse primer pair (Figure S1), sequenced, and backcrossed seven times to w^{1118} flies to generate an isogenized strain. The isogenized $vri^{\Delta 679}$ mutant was used to carry out all subsequent experiments.

*vri*70kb$^{\Delta E\text{-}Box}$ transgene construction and transgenic fly generation

BAC clone CH321-28E21 (BacPac Resources) was used to generate the *vri*70kb$^{\Delta E\text{-}Box}$ transgene. Initially the E-box-containing region of this BAC clone was sub-cloned into the TA vector (Invitrogen) using the following primers: *vri* E-box region Forward, 5' GTTCCTTCTCTCGAAGGACCACT 3'; *vri* E-box region Reverse, 5' GCTGGGGAGTTGGGAAAACTG 3'.

The resulting plasmid, *vri*Ebox-TA, was used to mutate the E-boxes using the QuickChange II XL site directed mutagenesis kit (Stratagene, La Jolla, CA). For each E-Box, the following complementary forward and reverse primers were used to generate the indicated deletion: *vri* E-box 1 mutation Forward, 5' GCTGGTGCCTCCACGAACCGCTCCGC 3'; *vri* E-box 1 mutation Reverse, 5' GGCTAGTGCAACGCTCCCCAACAGCC 3'; *vri* E-box 2&3 mutation Forward, 5' AATCGGGCGACTGATATCGCGCAG 3'; *vri* E-box 2&3 mutation Reverse, 5' TCCGGACCAATCGTAGTCGGATCCG 3'; *vri* E-box 4 mutation Forward, 5' CCCATCTGTCGATTTGTTCGTCGTAC 3'; *vri* E-box 4 mutation Reverse, 5' CGCTTTGAAACTTTGGATAGTTTAACAAGGGG 3'. E-box deletions in the resulting plasmid, *vri*ΔEbox-TA, were confirmed by sequencing. The E-box-containing region of the BAC clone was replaced by a selectable *galK* gene using bacterial homologous recombination (Warming et al., 2005). The *galK* gene was then replaced with an amplicon containing the E-box mutant region from *vri*ΔEbox-TA that was produced using the *vri* E-box GalK homology Forward (5' TTGGCTTGCGTAGCCGACTCAAGTCGCCAACATGTGAG CCGTCGCAGGCCCCTGTTGACAATTAATCATCGGCA 3') and *vri* E-box GalK homology Reverse (5' ATACGTACATATGTATATTTGAAGTTCCAATCAGTGAATT TTTGGGTTTCTCAGCACTGTCCTGCTCCTT 3') primers (Venken et al., 2008). We used primers containing ~50 bp homology arms when carrying out the homologous recombination (see Table 2). After selection of recombinants and sequence verification, the resulting *vri*70kb$^{\Delta E\text{-}Box}$ transgene was inserted at VK5, VK13 and VK20 docking sites via *PhiC32*-mediated recombination (Venken et al., 2006).

vri24 and *vri24*HA transgenes construction and transgenic fly generation

BAC clone CH322-102O15 (BacPac Resources) was used to generate the *vri24*kb and *vri24*HA transgenes. The *vri24*kb transgene is a 24kb BAC clone containing partial *vri* gene sequence

(chr2L5295134 - chr2L5319513) without any modifications. This transgene was inserted at the VK33 docking site via *PhiC32*-mediated recombination (Venken et al., 2006).

The *vri24*HA transgene has an N-terminal V5 and 3xHA epitope introduced to the *vri24*kb transgene using bacterial recombination (Venken et al., 2008). The V5-3xHA epitopes were inserted immediately downstream of the initiation codon of *vri*-ADF mRNA using a V5-3xHA recombination cassette comprised of the V5-3xHA epitope sequence, a *Kanamycin* (*Kan*) gene flanked by loxP sites, and two homology arms generated via PCR using the 'V5-3xHA-vri Homology Forward' and 'V5-3xHA-vri Homology Reverse' primers (Table 2). After selection for recombinants and sequence verification, the *Kan* cassette was removed using CRE recombinase as described (Venken et al., 2008). After sequence verification, the resulting *vri24*HA transgene was inserted at the VK20 docking site via *PhiC32*-mediated recombination (Venken et al., 2006).

RNA-seq library preparation

w^{1118} control and $vri^{\Delta 679}$ mutant flies were entrained for three days in LD at 25ºC. Flies were collected at ZT2 and ZT14, frozen on dry ice and heads were isolated as described (Oliver and Phillips, 1970). Total RNA from heads was extracted using TRIzol, treated with TURBO™ DNase (Thermo Fisher Scientific), precipitated and then purified with Lithium Chloride (Thermo Fisher Scientific) following manufacturer's instructions. A total of 1ug of RNA was used to isolate mRNA using the NEBNext Poly(A) mRNA Magnetic Isolation Module (New England Biolabs). RNA library construction was conducted using the NEBNext® Ultra™ II Directional RNA Library Prep Kit for Illumina (New England Biolabs) following the manufacturer's instructions. Libraries were sent to Texas A&M AgriLife Genomics and Bioinformatics Facility where they were mixed and multiplexed at the same equimolar concentrations and sequenced on a Hi-seq 2500 (Illumina) using 75bp single-end reads. The sequenced reads were mapped to the *Drosophila melanogaster* genome (dm6 – UCSC) with STAR aligner version 2.6.1d (Dobin et al., 2013).

Procedures to quantify and estimate differential expression were done as previously described (Pertea et al., 2016). Only genes that have an adjusted p-value ≤ 0.05 and fold change ≥ 1.5 (high expression) or ≤ 0.5 (low expression) were considered as differentially expressed genes in $vri^{\Delta 679}$ flies.

Drosophila activity monitoring and behavior analysis

All fly strains used in behavior experiments were backcrossed seven times to w^{1118} flies to minimize effects due to differences in genetic background. Locomotor activity was monitored using the *Drosophila* Activity Monitor (DAM) system (Trikinetics). One to three-day old male flies were placed in monitors, and activity was recorded for 3 days in 12:12 light-dark (LD) cycles and for 7 days in constant darkness (DD) at 25ºC. Analyses of period, power and rhythm strength during constant darkness (DD) was carried out using ClockLab (Actimetrics) software as previously described (Agrawal and Hardin, 2016).

Immunostaining

Fly tissues were processed for immunostaining as previously described (Houl et al., 2008), with minor modifications. Larval brains were dissected at the L3 stage and adult tissues were dissected 3-5 days after eclosion. Dissected tissues were fixed with 3.7% formaldehyde, washed and blocked in PAXD buffer (1X PBS, 5% BSA, 0.03% sodium deoxycholate, 0.03% tritonX100) with 5% donkey or goat serum for 1 hour, and incubated with primary and secondary antibodies diluted in PAXD buffer. The following primary antibodies were used: guinea pig anti-VRI GP3 1:25,000, rabbit anti-HA ab9110 (Abcam) 1:200, pre-absorbed rabbit anti-PER (a gift from Michael Rosbash Laboratory, Brandeis University). The following secondary antibodies were used at a 1:200 dilution: goat anti-rabbit Alexa 647 (Molecular Probes), goat anti-guinea pig Cy-3 (Jackson ImmunoResearch Laboratories, Inc.) as previously described (Liu et al., 2017).

Cryosectioning

Flies with a wild-type clock (w^{1118}) were sectioned into 10μM thickness sections and collected on Superfrost plus microscopic slides (Fisher Scientific). All sections were fixed with 3.7% formaldehyde for 15 minutes. Subsequent immunostaining steps were identical to those described for whole mount immunostaining.

Confocal microscopy and image analysis

Confocal imaging was carried out as described (Agrawal et al., 2017), with minor modifications. Fly tissues were imaged using an Olympus FV1000 confocal microscope 20x /0.8 NA or 100x /1.4 NA oil immersion objective lenses. Serial optical scans were obtained at 3 μM intervals (with 20x objective lens) Original Olympus images were saved as 12-bit oib format. Preliminary image processing was carried out using either FV1000 confocal software or Adobe Photoshop.

Western blotting

Western blot analyses were conducted as described (Zhou et al., 2016), with minor modifications. MTs were collected for protein extraction intact along with some contaminating intestinal tissue. Compound eyes were dissected as described (Zeng et al., 1994). After protein extraction, equal amounts of RIPA S extract were run, transferred, and probed with guinea pig anti-VRI GP3, 1:5,000, rabbit anti-HA, 1:5,000 and mouse anti-beta-actin (Abcam), 1:20,000. Horseradish peroxidase-conjugated secondary antibodies (Sigma) against guinea pig, rabbit and mouse were diluted 1:5,000. Immunoblots were visualized using ECL plus (GE) reagent.

RNA extraction, quantitative RT-PCR and data analysis

RNA extraction and quantitative RT-PCR was performed as described (Zhou et al., 2016), with minor modifications. Flies were entrained in 12:12 light-dark (LD) for at least 3 days, collected at

the indicated time points, and frozen. For RNA extracted from embryos, larvae and pupae all sub-stages were pooled together to represent all sub-stages. Total RNA was isolated and cDNA was synthesized using Superscript II (Invitrogen). The reverse transcription (RT) product was amplified with SsoFast qPCR Supermix (Bio-Rad) in a Bio-Rad CFX96 Real-Time PCR System using the following gene or transcript-specific primers: *vri*-ADF qPCR Forward, 5' ACGCTGGAACAGAAAGTGA 3'; *vri*-E qPCR Forward, 5' CATAACGACCAACGGCCG 3'; *vri*-ACDEF qPCR Reverse, 5' GCTAGTTTCTGCTGCAGTTG 3'; *vri* qPCR Forward, 5' ATGAACAACGTCCGGCTATC 3'; *vri* qPCR Reverse, 5' CTGCGGACTTATGGATCCTC 3'; *rp49* qPCR Forward, 5' TACAGGCCCAAGATCGTGAA 3'; *rp49* qPCR Reverse, 5' GCACTCTGTTGTCGATACCC 3'. For each sample, mRNA quantity was determined as described (Zhou et al., 2016). *rp49* mRNA levels were used as a normalization control when determining the relative levels of mRNA. Student two-tailed t-tests with unequal variances were performed to determine whether differences in levels were statistically significant. To evaluate the rhythmicity of *vri* isoform a One-Way ANOVA was conducted followed by a Tukey test for multiple comparison using the GraphPad Prism Software version 5.3 (Prism, La Jolla, CA) using as criteria to be considered rhythmic a p-value ≤ 0.05 and a significant difference in more than 2 timepoints ($p \leq 0.05$ based on the Tukey test comparing all timepoints).

S2 cell culture experiments

S2 cell maintenance was carried out as described with minor modifications (Mahesh et al., 2014). Cells were maintained in Schneider's Drosophila medium (Invitrogen) containing 10% fetal bovine serum with (100 units/ml) penicillin and streptomycin (100 µg/ml) (Invitrogen). S2 cells at 60–80% confluence were transiently transfected with C-terminally epitope tagged *vri*A-Flag-HA (FMO13008) or *vri*C-Flag-HA (FMO07976) using Effectene Transfection Reagent (Qiagen) (6.4 µL of Enhancer, 10 µL of Transfection Reagent, 0.8 µg of total DNA), and 24 hour after cells were collected for protein extractions as described for western blotting.

Supplemental References

AGRAWAL, P. & HARDIN, P. E. 2016. The Drosophila Receptor Protein Tyrosine Phosphatase LAR Is Required for Development of Circadian Pacemaker Neuron Processes That Support Rhythmic Activity in Constant Darkness But Not during Light/Dark Cycles. *J Neurosci,* 36**,** 3860-70.

AGRAWAL, P., HOUL, J. H., GUNAWARDHANA, K. L., LIU, T., ZHOU, J., ZORAN, M. J. & HARDIN, P. E. 2017. Drosophila CRY Entrains Clocks in Body Tissues to Light and Maintains Passive Membrane Properties in a Non-clock Body Tissue Independent of Light. *Curr Biol,* 27**,** 2431-2441 e3.

BLAU, J. & YOUNG, M. W. 1999. Cycling *vrille* expression is required for a functional *Drosophila* clock. *Cell,* 99**,** 661-71.

DOBIN, A., DAVIS, C. A., SCHLESINGER, F., DRENKOW, J., ZALESKI, C., JHA, S., BATUT, P., CHAISSON, M. & GINGERAS, T. R. 2013. STAR: ultrafast universal RNA-seq aligner. *Bioinformatics,* 29**,** 15-21.

EMERY, P., SO, W. V., KANEKO, M., HALL, J. C. & ROSBASH, M. 1998. CRY, a *Drosophila* clock and light-regulated cryptochrome, is a major contributor to circadian rhythm resetting and photosensitivity. *Cell,* 95**,** 669-79.

HOUL, J. H., NG, F., TAYLOR, P. & HARDIN, P. E. 2008. CLOCK expression identifies developing circadian oscillator neurons in the brains of Drosophila embryos. *BMC Neurosci,* 9**,** 119.

LIU, T., MAHESH, G., YU, W. & HARDIN, P. E. 2017. CLOCK stabilizes CYCLE to initiate clock function in Drosophila. *Proc Natl Acad Sci U S A,* 114**,** 10972-10977.

MAHESH, G., JEONG, E., NG, F. S., LIU, Y., GUNAWARDHANA, K., HOUL, J. H., YILDIRIM, E., AMUNUGAMA, R., JONES, R., ALLEN, D. L., EDERY, I., KIM, E. Y. & HARDIN, P. E. 2014. Phosphorylation of the transcription activator CLOCK regulates progression through a approximately 24-h feedback loop to influence the circadian period in Drosophila. *J Biol Chem,* 289**,** 19681-93.

MOSES, K., ELLIS, M. C. & RUBIN, G. M. 1989. The glass gene encodes a zinc-finger protein required by Drosophila photoreceptor cells. *Nature,* 340**,** 531-6.

OLIVER, D. & PHILLIPS, J. P. 1970. Technical note. *Drosophila Information Service,* 45**,** 58.

PERTEA, M., KIM, D., PERTEA, G. M., LEEK, J. T. & SALZBERG, S. L. 2016. Transcript-level expression analysis of RNA-seq experiments with HISAT, StringTie and Ballgown. *Nat Protoc,* 11**,** 1650-67.

VENKEN, K. J., HE, Y., HOSKINS, R. A. & BELLEN, H. J. 2006. P[acman]: a BAC transgenic platform for targeted insertion of large DNA fragments in D. melanogaster. *Science,* 314**,** 1747-51.

VENKEN, K. J., KASPROWICZ, J., KUENEN, S., YAN, J., HASSAN, B. A. & VERSTREKEN, P. 2008. Recombineering-mediated tagging of Drosophila genomic constructs for in vivo localization and acute protein inactivation. *Nucleic Acids Res,* 36**,** e114.

WARMING, S., COSTANTINO, N., COURT, D. L., JENKINS, N. A. & COPELAND, N. G. 2005. Simple and highly efficient BAC recombineering using galK selection. *Nucleic Acids Res,* 33**,** e36.

ZENG, H., HARDIN, P. E. & ROSBASH, M. 1994. Constitutive overexpression of the Drosophila period protein inhibits period mRNA cycling. *Embo J,* 13**,** 3590-8.

ZHOU, J. 2017. *Characterizing the function of CLOCKWORK ORANGE in the circadian feedback loops in Drosophila melanogaster.* Biology PhD, Texas A&M University.

ZHOU, J., YU, W. & HARDIN, P. E. 2016. CLOCKWORK ORANGE Enhances PERIOD Mediated Rhythms in Transcriptional Repression by Antagonizing E-box Binding by CLOCK-CYCLE. *PLoS Genet,* 12**,** e1006430.